This document is the accepted manuscript version of the following article:
Li, M., Xu, N., Zhang, J., Lou, R., Shi, M., Li, L., … Wang, S. (2021). Quantization of the band at the surface of charge density wave material 2H-TaSe2. Chinese Physics B, 30(4), 047305 (7 pp.).
https://doi.org/10.1088/1674-1056/abe9a8

Quantization of the band at the surface of Charge Density Wave material 2H-$TaSe_2$

Man Li,[1,2] Nan Xu,[3,4] Jianfeng Zhang,[2] Rui Lou,[5,2,6,7] Xin Gao,[8] M. Shi,[3] Lijun Li,[9,10] H. C. Lei,[2] Cedomir Petrovic,[10] Zhonghao Liu,[11] B.-B. Fu,[8] K. Liu,[2] Yaobo Huang,[1,*] and S.-C. Wang[2,†]

[1] *Shanghai Synchrotron Radiation Facility, Shanghai Institute of Applied Physics, Chinese Academy of Sciences, Shanghai 201204, China*
[2] *Department of Physics and Beijing Key Laboratory of Opto-electronic Functional Materials & Micro-nano Devices, Renmin University of China, Beijing 100872, China*
[3] *Swiss Light Source, Paul Scherrer Institute, CH-5232 Villigen, Switzerland*
[4] *Institute of Advanced Studies, Wuhan University, Wuhan 430072, China*
[5] *School of Physical Science and Technology, Lanzhou University, Lanzhou 730000, China*
[6] *State Key Laboratory of Surface Physics and Department of Physics, Fudan University, Shanghai 200433, China*
[7] *Collaborative Innovation Center of Advanced Microstructures, Nanjing 210093, China*
[8] *Beijing National Laboratory for Condensed Matter Physics, and Institute of Physics, Chinese Academy of Sciences, Beijing 100190, China*
[9] *Chongqing Technology and Busineee University, Chongqing 400067, China*
[10] *Condensed Matter Physics and Materials Science Department, Brookhaven National Laboratory, Upton, NY 11973, USA*
[11] *State Key Laboratory of Functional Materials for Informatics and Center for Excellence in Superconducting Electronics, SIMIT, Chinese Academy of Sciences, Shanghai 200050, China*

By using angle-resolved photoemission spectroscopy combined with the first-principles electronics atructure calculations, we report the quantum well states at the surface of a single crystal 2H-$TaSe_2$. We observed sub-bands at the three-dimensional Brillouin zone center forming the quantized states due to its highly dispersive nature and light effective mass along k_z direction. The quantized sub-bands shift upward towards E_F with the decrease of temperature across $T_{\rm CDW}$. The band shift could not be explained by two-dimensional Fermi-surface nesting-driven charge density waves(CDW), nor by purely strong electron-phonon coupling only. The CDW in 2H-$TaSe_2$ is likely related to the bands at higher binding energy, and the CDW mechanism could be explained by the excitons, and our observation gives support to this scenario.

I. INTRODUCTION

Manipulation of two-dimensional electron gas (2DEGS) has recently drawn considerable interest[1–4]. As a mechanism for tailoring the many-body interactions, 2DEGS was embodied in the interface of semiconductors [5–7], metal-films [8–10]. This has attracted a lot of interest due to observation of high electron mobility[11, 12], quantum Hall effect [13, 14], superconductivity [15] and large magnetoresistance [16], *etc.* In spite of the complicated and diverse microscopic origin, the 2DEGS are generally caused by the confinement of electrons along one dimension, for example, by the depletion of charge carriers close to the surface and then induce a band-bending to confine the electrons into 2DEGS [17]. Due to the shielding effect of good conductors, it is difficult to acheive 2DEG in metals. Monolayer transition metal dichalcogenides (TMDs) MX_2 (M = Mo, W; X = S, Se) represent a natural host for 2DEGS [18].

The CDW is a controversial topic in quasi-two-dimensional TMDs since their discovery over the past few decades. On one hand, neither a weak-coupling approach nor strong coupling mean-field models, *e.g.* the Fermi surface(FS) nesting [19–21], saddle point [22–24], local chemical bonds [25, 26], and excitonic insulator [27–29], can explain the driving mechanism of the CDW in TMDs. The presence of substantial lattice distortion in the ordered phase, however, also points to the significance of electronic-phonon coupling[30, 31]. On the other hand, there is coexistence or competition between the CDW and superconductivity [32, 33], in different crystal structures. Thus the mechanism of CDW remains a challenge.

2H-$TaSe_2$ is an interesting TMDs with the interplay of CDW and superconductivity when Se is substituted with S [32]. It consists of three-atom-thick chalcogen-transition metal-chalcogen sandwiches and its unit cell can be considered as two layers of Ta-Se with a 60° rotation with van der Waals' force in adjoining layers [32]. 2H-$TaSe_2$ undergoes a second-order transition from normal phase to an incommensurate ordered phase at T = 122 K, followed by a first-order lock-in transition to a 3×3 commensurate phase at $T_{\rm CDW}$ = 90 K. [32, 34] The CDW in 2H-$TaSe_2$ has been investigated experimentally by ARPES, STM, transport measurement, neutron scattering [20, 21, 34–43], and band structure calculations [44–46]. The susceptibility calculation from the low energy bands (or FSs) disagrees with the CDW wave vectors in TMDS and excludes the FS nesting as a driven force [31, 44]. The strong electron-phonon coupling with wave-vector-dependent electron-phonon matrix elements [47] and a new type of collective excitation [36] as the condensation of preformed excitons [48] are proposed, but further evidence is needed.

* huangyaobo@zjlab.org.cn
† scw@ruc.edu.cn

In this Letter, we report an ARPES study of the electronic structure of the 2H-$TaSe_2$ with various photon energies in both the compensate CDW state and normal state. In addition to the 2D-like band structure reported before, we observe a quantum well state induced by the intrinsic band structure at Brillouin zone center (Γ) below E_F in 2H-$TaSe_2$ single crystal for the first time. It is formed by a band adjacent to E_F present in the bulk band calculation but not in the ARPES measurement. The combination of near-surface band bending potential created by the rearrangement of surface electrons, which is mostly observed in semiconductors [17], and the light effective mass along k_z direction, cause the quantization along c-axis and formation of the 2D manifold sub-bands at the surface. With the decrease of temperature below $T_{\rm CDW}$, the 2D sub-bands shifted upward while other bands show no noticeable change. Both the pseudogap and the abnormal band shift in 2H-$TaSe_2$ could be explained by the model of Preformed Excitonic Liquid [48].

II. MATERIALS AND METHODS

Single crystals of 2H-$TaSe_2$ were grown by the iodine vapor transport method. The element analysis and transport measurement of samples indicate the high quality of crystals in this paper [32]. ARPES measurement was performed at the Dreamline beamline of the Shanghai Synchrotron Radiation Facility with a Scienta D80 analyzer and at the SIS-HRPES beamline of the Swiss Light Source with a Scienta R4000 analyzer. The energy and angular resolutions were better than 15 meV and 0.2°, respectively. The sample for the ARPES measurements are cleaved *in situ* along (001) direction in a vacuum better than 5×10^{-11} Torr. Normal and CDW phases measurements are taken at T = 150 K and T = 20 K, respectively. The electronic structure of 2H-$TaSe_2$ was studied by using first-principles calculations with the projector augmented wave (PAW) method [49, 50] as implemented in the VASP package [51–53]. For the exchange-correlation functional, the generalized gradient approximation (GGA) of the Perdew-Burke-Ernzerhof (PBE) formula [54] was adopted. The kinetic energy cutoff of the plane-wave basis was set to be 300 eV. A $16 \times 16 \times 4$ k-point mesh was utilized for the Brillouin zone (BZ) sampling and the Fermi surface was broadened by the Gaussian smearing method with a width of 0.05 eV. The vdW interactions between the $TaSe_2$ layers were considered by adopting the optB86b-vdW functional [55]. The lattice parameters and internal atomic positions were fully relaxed until the forces on all atoms were smaller than 0.01 V/ Å. After the equilibrium structures obtained, the electronic structures were calculated by including the spin-orbit-coupling (SOC) effect. In the slab calculation, a two-dimensional (2D) supercell with a 21-layer $TaSe_2$ slab and a 20-A vacuum was employed.

III. RESULTS AND DISCUSSION

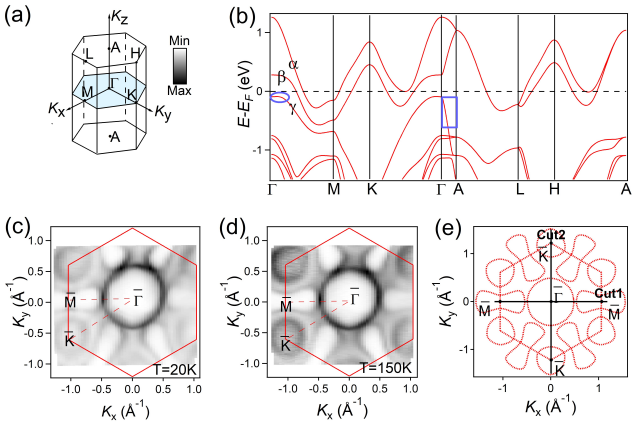

Figure 1. (Color Online) Brillouin zone and Fermi surface of 2H-$TaSe_2$. (a) 3D bulk BZ with marked high-symmetry points and a colored high symmetry plane. (b) Calculated bulk band structure along high-symmetry lines including SOC. Three near-E_F bands are denoted as α, β and γ, respectively. (c), (d) Integrated intensity plots within $E_F \pm 10$ meV at T = 20 K and 150 K to show the FS topology, obtained with $h\nu = 50$ eV showing the colored plane indicated in (a), corresponding to CDW and normal phase, respectively. (e) The extracted ARPES mapping in the normal state. Marked cuts # 1 and # 2 indicate the momentum locations of the measured bands in Fig. 3.

The schematic bulk BZ is presented in Fig. 1(a). We performed the band calculation along high symmetry lines of bulk, as shown in Fig. 1(b). Two Ta d bands, split by the bi-(Ta-Se) layers, labeled as α and β, crossing E_F along high symmetry lines are shown in Fig. 1(b) [44, 46]. Fig. 1(c) and Fig. 1(d) demonstrate the FS topologies of 2H-$TaSe_2$ at temperature below (T = 20 K) and above (T = 150 K) commensurate CDW transition temperature, respectively, with photon energy $h\nu =$ 50 eV. This corresponds to the Γ-M-K plane and is indicated as the color plane in Fig. 1(a). we observe the two hole-pockets centered at Γ and K, respectively, and a "dog-bone" shaped electron-pockets centered at M in the normal state (Fig.1(d)). A "pseudogap" of unclear origin has been reported at K-centered FS by the suppression of the spectral weight at $T \gg T_{CDW}$ [20, 21]. At the low temperature in the commensurate CDW (CCDW) state, as illustrated in Figs. 1(c), the K-pocket completely loses its weight at E_F, whereas the M-pocket is only partially gaped, forming triangular FS pockets. We extract the Fermi wave vectors from the ARPES experimental data above $T_{\rm CDW}$ and plot them in Fig. 1(e). Our FS data are in agreement with early studies [20, 21, 35, 56], excluding the finite energy resolution and thermal broadening effects.

The temperature dependence of the gaps are shown in

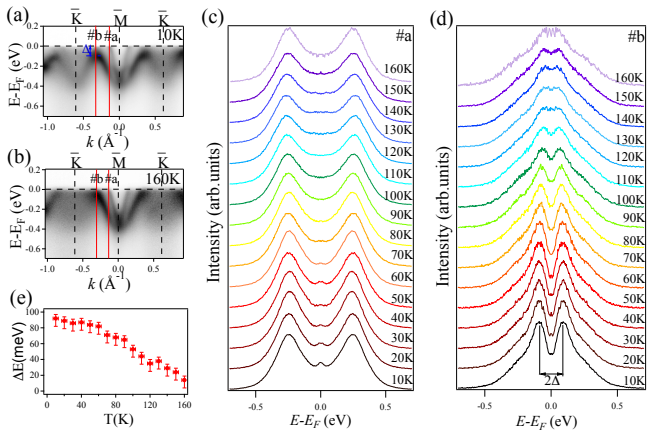

Figure 2. (Color online) Temperature dependence of band gap. (a) The band dispersion along the direction of K-M-K at $T = 10K$, Δ is the CDW gap. (b) Same as (a), but displayed at $T = 160K$. (c,d) The temperature dependence of symmetrized EDCs along the momentum marked by #a and #b, respectively. (e) The extracted band gap (Δ) as a function of temperature.

Fig. 2. Fig. 2(a) and Fig. 2(b) show the intensity plot along K-M-K at the CDW (T = 10 K) and normal state (T = 160 K), respectively. From the plots, we can see a band across E_F at #a, which forms the dog-bone shaped FS around M point both at the CDW and normal states, with no gap opening observed. For the band close to #b, which forms the circular FS around K point in Fig. 1, shows a clear bending back and a gap feature at low temperature, as shown in Fig. 2(a). At the normal state, the intensity becomes faint but the back bending and the gap feature remains. To illustrate the gap evolution, the symmetrized energy distribution curves (EDCs) at the crossing points are shown in Fig. 2(c) and Fig. 2(d) for crossing point #a and #b, respectively. For #a, the symmetrized EDCs show a small peak centered at E_F. The intensity decreases with the increase of temperature and diminishes at around 90 K. For #b, the symmetrized EDC shows a clear double peak feature at low temperature, suggesting a CDW gap of about $\sim 90 \pm 10$ meV. With the increase in temperature, the peak intensity decreases but the gap remains across the $T_{\rm CDW}$, forming a "pseudogap" up to room temperature. We extracted the full gap (2Δ) from the separation of two symmetrical quasiparticle (QP) peaks, and plotted the gap values at different temperatures in Fig 2(e). The maximum CDW gap 90±10 meV fits well in the previous STM measurements [39], decreases with temperature but persists above the $T_{\rm CDW}$.

The in-plane band dispersion along high symmetry directions are shown in Fig. 3. Two major momentum cuts (Γ-M and Γ-K) with photon energies h$\nu = 50$ eV ($k_z = 0$), indicated as cuts #1 and #2 in Fig. 1(e), are shown respectively. Along the Γ-M direction, we observed a hole-like band across E_F at both below and above the $T_{\rm CDW}$. According to the bulk band calculation, two bands (α, β) across E_F along Γ-M, and are nearly degenerate along A-L. From Fig. 3(a) and 3(b), the two bands are nearly degenerate and only become separable near M point at about $E_B \sim$ 300-400 meV. No observable change near E_F (band shifts or gap opening) is identified through the CDW transition along this direction. There has been reported a 3×3 reconstruction below $T_{\rm CDW}$ [21] in 2H-$TaSe_2$ and some faint shadow bands could be barely seen in the second derivative plots. The agreement between the ARPES results along Γ-K (3(f)–3(j)) and the bulk band calculation is similar as those along Γ-M, except the opening of CDW gap close to K point.

A major difference between the observation and the bulk band calculation is the existence of quantized states from the "missing" γ band which was not experimentally reported before. In the bulk band structure calculation [blue ellipse in Fig.1(b)], there is a hole-like band near the Brillouin zone center close to E_F. Instead, we observe several replica bands with the band top at about $E_B \approx$ 460 meV below E_F, which can be visualized from the 2D intensity plot (Fig. 3(a), 3(d), 3(f) and 3(i)) and the corresponding second derivative plot (3(b), 3(e), 3(g) and 3(j)). We attribute the quantized states to the surface bands caused by the breaking of translation symmetry along the c-axis, and the light effective mass of the band along this direction (Γ-A). The topmost few layers/vacuum interfaces could induce a spatial redistribution of carriers, leading to the bending of the electronic bands relative to the Fermi level, [17] and form a quantum well near the sample surface. To estimate the γ band dispersion along k_z, we plot the ARPES intensity data in Fig. 4(c), and estimate the band dispersion with the influence of quantization. The effective mass $m_z^* \approx 0.06\, m_e$ is extracted from a parabolic fit to the dispersion. We also note that the in-plane band mass estimated from the band dispersion along k_x and k_y are approximately $0.23m_e$ and $0.31m_e$, respectively, much higher than that along k_z. The surface quantizations are caused by downward shift of the near-surface band potential, which thus confine the *electronic-state-wavefunction* along k_z-direction, forming the 2D like quantized in-plane bands, similar to $SrTiO_3$, InN and $PtSe_2$ [2, 6, 57].

In order to study the band structure under the influence of surface band bending, we performed the band structure calculations with a 21-layer slab, and we plot the results along with high symmetry lines in Fig. 3(c) and 3(h), respectively. The slab calculation reproduces the sub-bands qualitatively in agreement with our experimental results. The separations of γ subbands are more pronounced than other bands, in agreement with the observations. This larger separation is due to the lower effective mass along the quantization dimension (c-axis), which can be seen from the dispersion along Γ–A in the bulk band calculation.

To quantitatively study the relationship between the band structure close to the Fermi level and the CDW

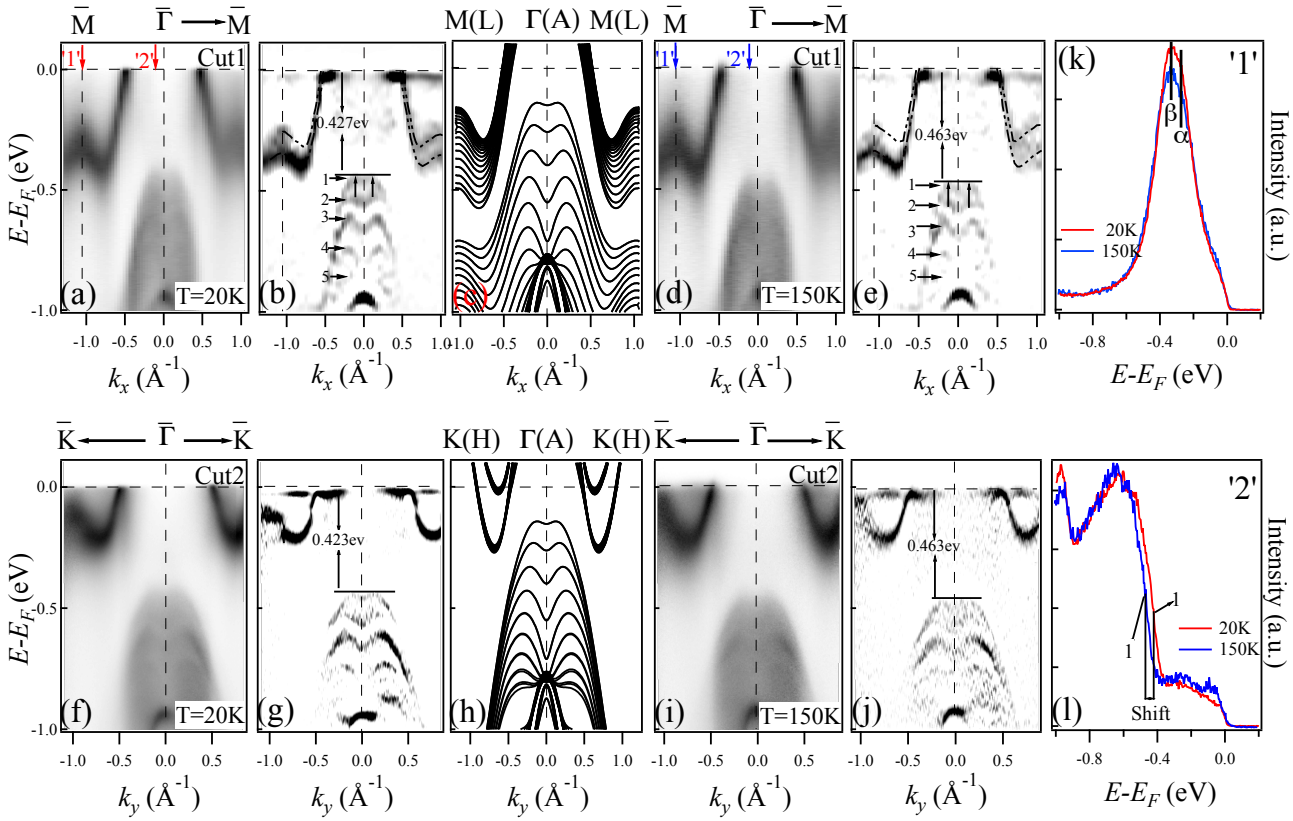

Figure 3. (Color online) Electronic structure along high-symmetry cuts. (a),(b) Intensity plot and the corresponding second derivative plot along the Γ-M direction (cut #1 in Fig. 1(e)) at T = 20 K, the black dotted-lines are guides to the eye. (c) slab calculation along Γ-M. (d),(e) Same as (a),(b), but recorded along the Γ-M direction at T = 150 K. (f),(g) Intensity plot and corresponding second derivative plot along Γ-K direction (cut #2 in Fig.1(e)) at T = 20 K. (h)Slab calculations along Γ-K. (i),(j) Same as (f),(g) recorded at T = 150 K. (k),(l) EDC plots in CDW and normal phase at the momentum marked by '1' and '2' in Fig .3(a) and Fig .3(d), respectively.

transition, we have traced the three bands, α, β and γ as noted in bulk band calculation in Fig. 1(b), to view their changes with temperature. The measured CDW/normal state band dispersions are illustrated in Fig. 3(a)/3(d) and Fig. 3(f)/3(i), along Γ-M and Γ-K, respectively. At the low temperature, in spite of the shadow bands caused by the 3×3 reconstruction and the opening of CDW gaps close to E_F along near K point, the bands show no noticeable energy shift compared with the normal state. In contrast, the quantized γ sub-bands, show down shifts with the temperature increase. The binding energy of the topmost sub-band shift downward about 30 meV, from $E_B \approx 427$ meV at T = 20 K to $E_B \approx 461$ meV at T = 150 K which is beyond the experimental resolution, and so are the following sub-bands. In order to compare the energy shift of the bands, we overlay the EDCs at below and above $T_{\rm CDW}$ at points marked as '1' and '2' in Fig. 3(a) and 3(d), and the comparisons are shown in Fig. 3(k) and Fig. 3(l), respectively. From Fig. 3(k), no energy shift is observed across the $T_{\rm CDW}$ for α and β bands at High symmetry M point, while the quantized sub-bands of γ show a clear shift with temperature changes.

We further perform the k_z-dependent measurements in ΓM–AL plane by varying the photon energy, covering more than one BZ along k_z. Fig. 4(a) shows the integrated spectra intensity plot around E_F as a function of k_x and k_z, defined as cut #1 in Fig. 1(e). The α, β bands are nearly degenerate and show little dispersion along k_z, suggesting 2D like characters of the bands. We also show the band dispersion along M–L and Γ–A, labeled as cut #3 and cut #4, in Fig. 4(b) and 4(c), respectively. The k_z value was converted with the inner potential V_0 = 17 eV empirically to best fit the dispersion. Fig. 4(b) shows the ARPES intensity plot along the M–L line, the "dips" and "peaks" of the band structures confirm the periodic variation of electronic states. The insets show EDCs at high symmetry points (i.e. M and L), with the splitting of α and β bands at M and nearly degenerate at L, in agreement with the bulk band calculation shown in Fig. 1(b).

Fig. 4(c) shows the intensity plot along the Γ–A–Γ line over more than two BZs. Besides the flat dispersionless

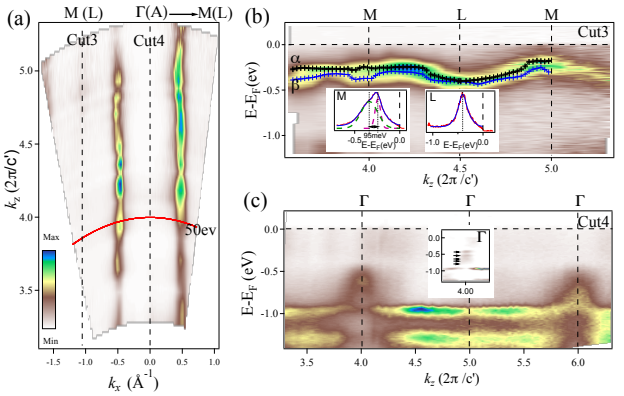

Figure 4. (Color online) Photon-energy-dependent band dispersion of 2H-$TaSe_2$. (a)integrated ARPES intensity map within $E_F \pm$ 10 meV in the $h\nu - k_{\|}$ plane , where $k_{\|}$ is oriented along the Γ-M (A-L) direction, recorded with various photon energies. (b) ARPES intensity plot along the $M - L$ direction, from cut #3 in Fig. 4(a), the markers are guide to eyes. Insets show multiple Guassian peaks fit to the EDCs at high symmetry points M and L, respectively. (c) ARPES intensity plot along the $\Gamma - A$ direction, cut #4, taken with photon energies covering a k_z range over 2 BZs. Inset shows a zoom in second derivative plot at Γ point.

band located about 1 eV below E_F, the most striking feature is a dispersive band around Γ, with an energy range between 0.5–0.9 eV. Closer investigation shows quantized energy levels around Γ, with the band top about 430–460 meV below E_F, in agreement with the in-plane observations. Due to the existence of quantized states, we can only roughly estimate the band dispersion and extract the band mass along k_z direction $m_z^* \approx 0.06 m_e$, much lighter than those in-plane values. Hence, in consideration of the photon-energy dependence, the dispersions of 2H-$TaSe_2$ is strong. Most of the time, the 2H-$TaSe_2$ was considered as a quasi-2D system, and the CDW is studied in a two-dimensional approach. Our data suggest that a simple two-dimensional approximation may not be sufficient.

It has been a long-standing puzzle that the γ band is absent and only two hole-like bands centered in BZ center are observed in. For a band with fast dispersion and light effective mass along the c-axis, the band bending effect, which is caused by the breaking of translation symmetry at the surface, will make the quantization more observable and hinder the observation of the bulk band. From the bulk band calculation (Fig. 1(b)), in comparison with other bands, the γ band disperses rapidly along Γ–A, with relatively flat in-plane dispersion and higher effective mass. To quantitatively study the surface quantization, the slab calculation with 21 layers of $TaSe_2$ and the band dispersions are shown in Fig. 3(c) and 3(h), respectively. With the quantization, the quantum well states are located at higher binding energies than the bulk band calculation, in agreement with the experimental observation. In contrast, the quantization of α, β bands are not as clear as of γ band due to slower dispersion and higher effective mass along the c–axis. This can be seen from the less separation of the states in the slab calculations. From the comparison between the bulk band and the slab calculations, in addition to the consistency between ARPES measurement and slab calculation, we safely "recover a missing" bulk band in 2H-$TaSe_2$ as an isotropic, a near flat in-plane band close E_F centered on 3D BZ center, with fast dispersion along k_z.

The mechanism of CDW in TMDs remains a puzzle due to its complexity. The weak coupling 2D FS-nesting assumption has failed since there is no clear connection of FSs with the CDW vector ($Q_{\mathrm{CDW}} = \frac{2}{3}\Gamma\mathrm{M}$). FS nesting with 3D wave vector is proposed to explain the CDW in VSe_2 with a sizable variation of bands along k_z [58, 59]. Exciton condensation has been applied to understand the CDW in 1T- $TiSe_2$ [29, 60]. Strong electron-phonon coupling[47] and scattering between saddle points were proposed to understand the mechanism in 2H- $TaSe_2$ [22–24], but pseudogap [20, 21], quasiparticle self-energy[36],and temperature dependent dc resistivity[34, 43] are still not fully understood. Preformed excitonic liquid theory explained the aforementioned physics well, but the lack of any signature of carrier-lattice coupling in previous ARPES suggests that the CDW is dominantly electronically driven in 2H-$TaSe_2$ [48].

In our observation, during the CDW transition (T_{CDW} = 90 K), the band positions of α, β bands remain stable within the energy resolution. In contrast, the quantized γ sub-bands shift about 30 meV across the transition temperature. This shift could not be due to a thermal effect or chemical shift for the relatively stable positions of α, β bands, and the value of 30 meV is beyond the system resolution ($\Delta E \leq$ 15 meV). The CDW ordered state in 2H-$TaSe_2$ has been interpreted as a Bose-condensed phase of excitons, and the shift might be the signature of excitonic coherence in the CDW states. When the preformed exciton in normal state condenses and becomes coherent, the excitonic interaction push γ band upward. This is in contrast to the weakly interacting FS scenario and pure strong electron-phonon coupling picture. At low temperature, DMFT calculation demonstrated an enhanced coherence with weak shoulder-like feature around 0.4 eV [48], which conforms to our ARPES scale where actually the shift happens and consistent with our observation. Our result is also not in conflict with the exciton-plus-phonon idea either [27, 28].

If we "recover" the bulk γ band from the observation and bulk band calculation, it would be located around E_F with relatively flat in-plane dispersion around BZ center. Since the γ band responses with the CDW transition, it could be its driving force. FS nesting occurs when the band is close to E_F, and if the "recovered" γ band in bulk is located near Fermi energy as indicated by electronic structure calculation, the high in-plane density of state could be a source of instability, driving the CDW transition. This scenario is unlikely because a CDW gap

or CDW induced down-shift of band is not observed, but an inverse of upward shift. One possible scenario that could cause an upward shift in CDW phase is the excitonic interaction between two bands where the valence band and the conduction band interact with a shift of certain wave vector [60]. The formation of CDW in excitonic phase is a process of a gradual buildup of excitonic coherence. It is accompanied with a decrease of band gap E_G by the shift of valence or/and conduction band, which become smaller than the binding energy of the exciton state E_B, causing an instability in the normal state [29, 56, 60]. In order to fully understand the CDW phenomenon, further detailed study of the electron, phonon structures, and the excitonic character of the TMDs are needed.

IV. CONCLUSION

In conclusion, we have observed quantized 2DEGs in single crystal 2H-$TaSe_2$ for the first time. We studied the in-plane and k_z dependence of the band dispersion and found out the quantization from a previous "missing" band, which is close to Fermi energy in Γ-M-K plane and highly dispersive along k_z. That quantization at the surface results from the band bending due to the surface electron rearrangement and the light carriers' effective mass of the band along Γ-A direction. The band shifts upward with the decrease of temperature into the CCDW state. The unusual shift is mostly related to the CDW transition. Based on the shift of the surface bands, we provide an evidence of excitonic interaction as the driving mechanism of the CDW in 2H-$TaSe_2$.

ACKNOWLEDGEMENTS

The authors thank Qiang Han for valuable discussions. This work was supported by the National Natural Science Foundation of China (Grants No. 11774421, No. 11774424, No. 11574394, No. 11774423, No. 11822412 and No. 11874047), the Ministry of Science and Technology of China (2016YFA0401002 and 2018YFA0307000), the National Key R&D Program of China (Grants No. 2016YFA0300504 and Grant No. 2018FYA0305800). N.X. was supported by "the Fundamental Research Funds for the Central Universities" (Grant No. 2042018kf-0030). Y.H. was supported by the CAS Pioneer Hundred Talents Program(type C). Work at Brookhaven National Laboratory was supported by US DOE, Office of Science, Office of Basic Energy Sciences (DOEBES), under Contract No. DE-SC0012704 (materials synthesis). M.L., X.N., and J.-F.Z.contributed equally to this work.

[1] A. F. Santander-Syro, O. Copie, T. Kondo, F. Fortuna, S. Pailhes, R. Weht, X. G. Qiu, F. Bertran, A. Nicolaou, A. Taleb-Ibrahimi, P. LeFvre, G. Herranz, M. Bibes, N. Reyren, Y. Apertet, P. Lecoeur, A. Barthélémy, and M. J. Rozenberg, Nature **469**, 189 (2011).
[2] W. Meevasana, P. D. King, R. H. He, S. K. Mo, M. Hashimoto, A. Tamai, P. Songsiriritthigul, F. Baumberger, and Z. X. Shen, Nature Materials **10**, 114 (2011).
[3] N. C. Plumb, M. Salluzzo, E. Razzoli, M. Månsson, M. Falub, J. Krempasky, C. E. Matt, J. Chang, M. Schulte, J. Braun, H. Ebert, J. Minár, B. Delley, K.-J. Zhou, T. Schmitt, M. Shi, J. Mesot, L. Patthey, and M. Radović, Physical Review Letters **113**, 086801 (2014).
[4] Z. Wang, S. McKeown Walker, A. Tamai, Y. Wang, Z. Ristic, F. Y. Bruno, A. De La Torre, S. Riccò, N. C. Plumb, M. Shi, P. Hlawenka, J. Sánchez-Barriga, A. Varykhalov, T. K. Kim, M. Hoesch, P. D. King, W. Meevasana, U. Diebold, J. Mesot, B. Moritz, T. P. Devereaux, M. Radovic, and F. Baumberger, Nature Materials **15**, 835 (2016).
[5] S. Abe, T. Inaoka, and M. Hasegawa, Physical Review B **66**, 205309 (2002).
[6] P. D. C. King, T. D. Veal, and C. F. McConville, Physical Review B **77**, 125305 (2008).
[7] P. D. C. King, T. D. Veal, C. F. McConville, J. Zúñiga-Pérez, V. Muñoz-Sanjosé, M. Hopkinson, E. D. L. Rienks, M. F. Jensen, and P. Hofmann, Physical Review Letters **104**, 256803 (2010).
[8] T. Hirahara, T. Nagao, I. Matsuda, G. Bihlmayer, E. V. Chulkov, Y. M. Koroteev, and S. Hasegawa, Physical Review B **75**, 035422 (2007).
[9] I. Matsuda, T. Ohta, and H. W. Yeom, Physical Review B **65**, 085327 (2002).
[10] N. Nagamura, I. Matsuda, N. Miyata, T. Hirahara, S. Hasegawa, and T. Uchihashi, Physical Review Letters **96**, 256801 (2006).
[11] A. Ohtomo and H. Y. Hwang, Nature **427**, 423 (2004).
[12] S. Thiel, Science **313**, 1942 (2006).
[13] K. V. Klitzing, G. Dorda, and M. Pepper, Physical Review Letters **45**, 494 (1980).
[14] D. C. Tsui, H. L. Stormer, and A. C. Gossard, Physical Review Letters **48**, 1559 (1982).
[15] N. Reyren, S. Thiel, A. D. Caviglia, L. F. Kourkoutis, G. Hammerl, C. Richter, C. W. Schneider, T. Kopp, A.-S. Ruetschi, D. Jaccard, M. Gabay, D. A. Muller, J.-M. Triscone, and J. Mannhart, Science **317**, 1196 (2007).
[16] A. Brinkman, M. Huijben, M. van Zalk, J. Huijben, U. Zeitler, J. C. Maan, W. G. van der Wiel, G. Rijnders, D. H. A. Blank, and H. Hilgenkamp, Nature Materials **6**, 493 (2007).
[17] Z. Zhang and J. T. Yates, Chemical Reviews **112**, 5520 (2012).
[18] J. G. Roch, G. Froehlicher, N. Leisgang, P. Makk, K. Watanabe, T. Taniguchi, and R. J. Warburton, arXiv:1807.06636 (2018).
[19] D. W. Shen, B. P. Xie, J. F. Zhao, L. X. Yang, L. Fang, J. Shi, R. H. He, D. H. Lu, H. H. Wen, and D. L. Feng, Physical Review Letters **99**, 216404 (2007).
[20] S. V. Borisenko, A. A. Kordyuk, A. N. Yaresko, V. B. Zabolotnyy, D. S. Inosov, R. Schuster, B. Büchner,

R. Weber, R. Follath, L. Patthey, and H. Berger, Physical Review Letters **100**, 196402 (2008).
[21] Y. W. Li, J. Jiang, H. F. Yang, D. Prabhakaran, Z. K. Liu, L. X. Yang, and Y. L. Chen, Physical Review B **97**, 115118 (2018).
[22] T. Rice and G.K. Scott, Phys. Rev. Lett. **35**, 120 (1975).
[23] R. Liu, C. G. Olson, W. C. Tonjes, and R. F. Frindt, Physical Review Letters **80**, 5762 (1998).
[24] R. Liu, W. C. Tonjes, V. A. Greanya, C. G. Olson, and R. F. Frindt, Physical Review B - Condensed Matter and Materials Physics **61**, 5212 (2000).
[25] M. H. Whangbo and E. Canadell, Journal of the American Chemical Society **114**, 9587 (1992).
[26] W. L. McMillan, Physical Review B **16**, 643 (1977).
[27] J. van Wezel, P. Nahai-Williamson, and S. S. Saxena, Physical Review B **81**, 165109 (2010).
[28] J. van Wezel, P. Nahai-Williamson, and S. S. Saxena, EPL (Europhysics Letters) **89**, 47004 (2010).
[29] H. Cercellier, C. Monney, F. Clerc, C. Battaglia, L. Despont, M. G. Garnier, H. Beck, P. Aebi, L. Patthey, H. Berger, and L. Forró, Physical Review Letters **99**, 146403 (2007).
[30] D. S. Inosov, V. B. Zabolotnyy, D. V. Evtushinsky, A. A. Kordyuk, B. Büchner, R. Follath, H. Berger, and S. V. Borisenko, New Journal of Physics **10**, 125027 (2008).
[31] M. D. Johannes and I. I. Mazin, Physical Review B **77**, 165135 (2008).
[32] L. Li, X. Deng, Z. Wang, Y. Liu, M. Abeykoon, E. Dooryhee, A. Tomic, Y. Huang, J. B. Warren, E. S. Bozin, S. J. L. Billinge, Y. Sun, Y. Zhu, G. Kotliar, and C. Petrovic, npj Quantum Materials **2**, 11 (2017).
[33] S. Qiao, X. Li, N. Wang, W. Ruan, C. Ye, P. Cai, Z. Hao, H. Yao, X. Chen, J. Wu, Y. Wang, and Z. Liu, Physical Review X **7**, 041054 (2017).
[34] V. Vescoli, L. Degiorgi, H. Berger, and L. Forró, Physical Review Letters **81**, 453 (1998).
[35] K. Rossnagel, E. Rotenberg, H. Koh, N. V. Smith, and L. Kipp, Physical Review B **72**, 121103(R) (2005).
[36] T. Valla, A. V. Fedorov, P. D. Johnson, J. Xue, K. E. Smith, and F. J. DiSalvo, Physical Review Letters **85**, 4759 (2000).
[37] D. E. Moncton, J. D. Axe, and F. J. DiSalvo, Physical Review B **16**, 801 (1977).
[38] R. L. Withers and L. A. Bursill, Physical Review B **26**, 1469 (1982).
[39] C. Wang, B. Giambattista, C. G. Slough, R. V. Coleman, and M. A. Subramanian, Physical Review B **42**, 8890 (1990).
[40] J. A. Galvis, P. Rodière, I. Guillamon, M. R. Osorio, J. G. Rodrigo, L. Cario, E. Navarro-Moratalla, E. Coronado, S. Vieira, and H. Suderow, Physical Review B **87**, 094502 (2013).
[41] J. Demsar, L. Forró, H. Berger, and D. Mihailovic, Physical Review B **66**, 041101(R) (2002).
[42] D. V. Evtushinsky, A. A. Kordyuk, V. B. Zabolotnyy, D. S. Inosov, B. Büchner, H. Berger, L. Patthey, R. Follath, and S. V. Borisenko, Physical Review Letters **100**, 236402 (2008).
[43] B. Ruzicka, L. Degiorgi, H. Berger, R. Gaál, and L. Forró, Physical Review Letters **86**, 4136 (2001).
[44] J. Laverock, D. NewbyJr, E. Abreu, R. Averitt, K. E. Smith, R. P. Singh, G. Balakrishnan, J. Adell, and T. Balasubramanian, Physical Review B **88**, 035108 (2013).
[45] R. L. Barnett, A. Polkovnikov, E. Demler, W.-G. Yin, and W. Ku, Physical Review Letters **96**, 026406 (2006).
[46] Y. Ge and A. Y. Liu, Physical Review B **86**, 104101 (2012).
[47] L. P. Gor'kov, Physical Review B **85**, 165142 (2012).
[48] A. Taraphder, S. Koley, N. S. Vidhyadhiraja, and M. S. Laad, Physical Review Letters **106**, 236405 (2011).
[49] G. Kresse and D. Joubert, Physical Review B **59**, 1758 (1999).
[50] P. E. Blöchl, Physical Review B **50**, 17953 (1994).
[51] G. Kresse and J. Furthmüller, Computational Materials Science **6**, 15 (1996).
[52] G. Kresse and J. Hafner, Physical Review B **47**, 558 (1993).
[53] G. Kresse and J. Furthmüller, Physical Review B **54**, 11169 (1996).
[54] J. P. Perdew, K. Burke, and M. Ernzerhof, Physical Review Letters **77**, 3865 (1996).
[55] J. Klimeš, D. R. Bowler, and A. Michaelides, Journal of Physics: Condensed Matter **22**, 022201 (2010).
[56] K. Rossnagel, Journal of Physics: Condensed Matter **23**, 213001 (2011).
[57] O. J. Clark, F. Mazzola, J. Feng, V. Sunko, I. Marković, L. Bawden, T. K. Kim, P. D. C. King, and M. S. Bahramy, Physical Review B **99**, 045438 (2019).
[58] V. N. Strocov, M. Shi, M. Kobayashi, C. Monney, X. Wang, J. Krempasky, T. Schmitt, L. Patthey, H. Berger, and P. Blaha, Physical Review Letters **109**, 086401 (2012).
[59] K. Terashima, T. Sato, H. Komatsu, T. Takahashi, N. Maeda, and K. Hayashi, Physical Review B **68**, 155108 (2003).
[60] W. Kohn, Physical Review Letters **19**, 439 (1967).